Comparison of CH··O, SH··O, Chalcogen, and Tetrel Bonds Formed by Neutral and Cationic Sulfur-Containing Compounds

Steve Scheiner*
Department of Chemistry and Biochemistry
Utah State University
Logan, UT 84322-0300

ABSTRACT

The ability of neutral and charged S-compounds to form different sorts of noncovalent bonds is examined by ab initio calculations. Neutrals are represented by CH_3SH and fluorosubstituted $FSCH_3$; cations are $(CH_3)_3S^+$, $CH_3SH_2^+$, and $FHSCH_3^+$. Each is paired with N-methylacetamide (NMA) whose O atom serves as common electron donor. Charged species engage in much stronger noncovalent bonds than do the neutral molecules, by as much as an order of magnitude. The strongest noncovalent bond for any system is a O··SF chalcogen bond wherein the O lies directly opposite a S-F covalent bond, amounting to as much as 39 kcal/mol. Second in binding energy is the SH··O H-bond which can be as large as 34 kcal/mol. Somewhat weaker is the O··SC chalcogen bond, followed by the CH··O H-bond and finally the O··C tetrel bond, which has the appearance of a trifurcated H-bond. Any CH group which participates in a CH··O H-bond shifts its NMR signal downfield by an amount which is roughly proportional to the strength of the H-bond. This situation is clearly distinguishable from that in a O··S chalcogen or SH··O H-bond wherein the methyl protons are shifted upfield.

*steve.scheiner@usu.edu

keywords: NBO; AIM; NMR; trifurcated H-bond

INTRODUCTION

The notion of attractive forces existing between molecules is nearly as old as chemistry itself. In order to differentiate them from the covalent bonds that bind together the atoms within a molecule, these intermolecular forces are frequently referred to as noncovalent bonds. Of the various noncovalent bonds, the H-bond (HB) is arguably the most important and prevalent. It is traditionally formulated as the positioning of two molecules such that the H atom of one molecule, A-H, acts as a bridge to an atom D of another molecule. Although its earliest conception considered only highly electronegative atoms like O, F, and N as donor and acceptors [1-3], this picture has broadened considerably over recent years [4-17]. For example, despite some early resistance to the idea, the S atom is now recognized as a legitimate proton donor atom [18-23]. Also among those atoms which are now known to serve as proton donor is C, despite its nominally low electronegativity [24-34]. Carbon can overcome this limitation in several ways, one of which is to adopt a sp-hybridization which increases the polarity of the C-H bond. The attachment of an electron-withdrawing group to C can also enhance the partial positive charge on the CH proton.

In addition to H, other atoms can also serve a similar function as bridge between two molecules. Even a strongly electronegative halogen atom can interact attractively with an electron donor [35-47]. This attraction is facilitated by an anisotropic distribution of charge around the halogen (X) atom within a R-X bond. Although the partial charge on the X atom is typically negative overall, detailed examination of the potential around this atom reveals a small region of positive charge density, usually directly opposite the R-X bond. It is this region that can be attracted to an electronegative atom on the partner molecule in what has come to be called a halogen bond. The Coulombic attraction is supplemented by a strong dose of charge transfer from the electron donor to the σ*(R-X) antibonding orbital, precisely analogous to the HB transfer into the σ*(R-H) orbital which manifests as the stretching of the RH bond, and the red shift of its stretching frequency. Work over the years has shown that this bonding mechanism is not limited to the halogen family but extends as well to other atoms, some less electronegative than others [48]. Depending upon the column of the periodic table to which the bridging atom belongs, these noncovalent bonds have been denoted as chalcogen (6A) [49-55], pnicogen (5A) [17, 56-58\59-62], and tetrel (4A) [63-70] bonds.

A rapidly escalating body of work has probed the underlying nature of these various bonds, uncovering differences as well as similarities. One general conclusion arising from these studies is that the halogen, chalcogen, pnicogen, and tetrel bonds all have the capability to be rather strong, competitive with the more traditional HBs. All are affected by such factors as the identity of the bridging atom, as well as its substituents, the geometrical arrangement of the electron donor and acceptor units, and any charge on one species or the other. It has thus not been possible to make any overgeneralized statements about relative stability like, for example, any H-bond is stronger than a halogen bond, or even that a OH··O HB is necessarily stronger than CH··O HB.

The occurrence of CH··O H-bonds in biological structure and function is becoming increasingly well recognized [71-76]. A family of lysine methyltransferases provides just one important example. A cofactor of this enzyme is S-adenosyl-L-methionine (AdoMet) [77-80] which contains a cationic trivalent S atom, flanked on two sides by alkyl groups and on the third by a methyl, as illustrated in Scheme 1. Aided by the positive charge, it is thought that CH··O HBs formed by methyl or CH_2 groups neighboring the S atom are essential interactions in the catalytic activity of these enzymes. It is important to remember,

however, that a single, nearly linear CH··O HB of a methyl group can be difficult to distinguish from a tetrel bond, wherein the electron donor approaches the methyl group along a direction opposite the S-C bond, which would have the appearance of a trifurcated HB. Yet for all its similarity, a tetrel bond has some important differences with a CH··O HB, whether single or trifurcated. From a functional standpoint, such a tetrel interaction may represent a precursor of sorts to the S_N2 methyl transfer reaction in this family of enzymes.

It is not only the methyl group of AdoMet which can function as an electron acceptor, but the S atom as well, in what has come to be called a chalcogen bond. The H atom of a S-methyl group may lie fairly close to the S atom itself. The positioning of the electron donor group may thus be such as to make it hard to tell whether one is looking at a CH··O HB or a S··O chalcogen bond, or some combination of these two. The possibility of a chalcogen bond raises another possibility. When one of the substituents on the S atom, let us call it X, is electronegative, a O··S-X chalcogen bond, where the O donor approaches opposite the S-X covalent bond, is likely to differ from an approach opposite a S-C bond. And indeed, the S of AdoMet is flanked not only by a simple methyl, but by two alkyl groups of differing electronegativity. Added to this set of possibilities, a SH group has the potential to serve as a proton donor in a SH··O HB. An additional layer of complexity is associated with the charge on the S-species: a cationic electron acceptor is likely to be considerably more potent than a neutral species, probably strengthening all of the interactions above.

One is thus left with a dilemma in analyzing the quantitative contributions of various bonds to the stability of a particular structure, and even more so in predicting the optimal arrangement of a cofactor like AdoMet within the confines of a protein. Quantum calculations can be of immense helpfulness in disentangling some of these issues. The complications arising from the geometric restraints of a large macromolecule can be avoided by considering a pair of separate molecules, able to move freely in space. Each sort of noncovalent bond can be treated individually, evaluating not only the binding energetics but also the fundamental factors that contribute to each sort of bond. One can also determine the geometric aspects of an optimal arrangement for each bond. As an aid in deciphering the bonding patterns in experimental structures of macromolecules, the spectroscopic signature of each sort of bond can be elucidated.

This work addresses the intermolecular interactions of alklylated sulfur-containing compounds, both cationic and neutral. The trialkylated $(CH_3)_3S^+$ serves as a prototype of the AdoMet sulfone cofactor mentioned above, wherein S is bound to three alkyl groups. As such, it is capable of forming not only CH··O HBs, but also an O··S chalcogen bond. Since the geometry of $(CH_3)_3S^+$ makes it difficult to study these two sorts of interactions in complete isolation from one another (see below), two of the methyl groups were replaced by H which alleviates this problem, while also permitting examination of a possible SH··O HB as an alternative. Replacing one of the H atoms of $CH_3SH_2^+$ by F allows examination of the effects on all of these bonds of increased electron withdrawing power of one of the S-substituents. The effect of charge was pursued by consideration of the neutral analogues CH_3SH and $FSCH_3$. So as to ensure consistency, a common electron donor was chosen: N-methylacetamide (NMA) due to its similarity to a protein peptide group.

COMPUTATIONAL DETAILS

Ab initio calculations were carried out with the Gaussian-09 [81] suite of programs. Geometries were optimized and binding energies evaluated using the aug-cc-pVDZ basis set in conjunction with MP2

means of incorporating electron correlation. Binding energies were defined as the difference between the energy of the complex and the sum of the monomers, in their optimized geometries, and were corrected for basis set superposition error via the counterpoise [82] procedure. The presence of noncovalent bonds was elucidated in two complementary manners. Quantitative assessments of charge transfer between individual orbitals were made via the natural bond orbital (NBO) method [83-84], as implemented in the Gaussian-09 software. Atoms in Molecules (AIM) procedures [85-86] led to the elucidation of bonding paths between atoms, and the electron density at bond critical points, as an alternate approximation of bond strength.

Two neutral molecules were considered as electron acceptor, $SHCH_3$ and $SFCH_3$. Three cationic species were examined: $S(CH_3)_3^+$, $SH_2CH_3^+$, and $SHFCH_3^+$. N-methylacetamide (NMA) was used as the common electron donor, specifically its O atom. Each electron acceptor was placed initially in a position where it might form one of several types of attractive interaction with the O atom of NMA, and the entire geometry optimized. Categories of noncovalent bond considered were H-bonds, of either CH··O or SH··O type, and chalcogen bonds between S and the O of NMA. Finally a tetrel bond was evaluated, wherein the NMA O atom approaches the C of a methyl group directly along its local C_3 axis, in what might be described, at least geometrically, as a trifurcated set of three CH··O H-bonds. Not all types of noncovalent bonds resulted in a true minimum in which case certain geometric restrictions were imposed, as described in detail below.

RESULTS

$S(CH_3)_3^+$

In the case of $S(CH_3)_3^+$ the fully optimized O··S chalcogen bond geometry with NMA contains a R(O··S) distance of 2.849 Å. The binding energy of this structure is 19.81 kcal/mol, as indicated by the first entry in Table 1. Fig 1a shows that the methyl group lying opposite the O atom makes a θ(O··SC) angle of 174.4°, maximizing the overlap between the O lone pairs and the σ*(SC) antibonding orbital. However, the attraction cannot be attributed purely to the chalcogen bond as two of the CH hydrogen atoms lie only 2.23 Å from the O, permitting the formation of CH··O HBs. These HBs are confirmed by NBO analysis of this structure. As reported in the first column of Table 2, the NBO value of the perturbation energy E(2) corresponding to the $O_{lp} \rightarrow \sigma^*(SC)$ is 2.16 kcal/mol, whereas each CH··O HB contains a contribution of 2.45 kcal/mol.

There are several ways in which the methyl groups of $S(CH_3)_3^+$ can engage in a HB with NMA. The most stable such structure is a trifurcated geometry wherein one H from each methyl group comes within 2.2 Å of the NMA O atom. This trifurcated structure in Fig 1b is bound by 20.55 kcal/mol, the global minimum on this potential energy surface. NBO analysis reveals a combined 14.67 kcal/mol E(2) from the charge transfer in these three HBs. However, these three HBs are rather bent, with CH··O angles deviating from linearity by more than 30°. How might this trifurcated structure compare with one containing a single linear HB? Calculations revealed that a structure of the latter sort does not represent a minimum on the surface of this heterodimer. In order to make this comparison, it was necessary to enforce CH··O linearity during the optimization. The resulting geometry is illustrated in Fig 1c to have a R(O··H) distance of 1.909 Å, and is some 4 kcal/mol less stable than the trifurcated global minimum. NBO analysis of this configuration leads to a charge transfer energy of 12.56 kcal/mol, with a small addition arising from the H atom of a second methyl group.

One might envision another H-bonded structure, wherein three different H atoms approach the NMA O, but unlike geometry 1b, all three H atoms are part of the same methyl group. Indeed, such a structure was found to represent a true minimum on the potential energy surface, and is illustrated in Fig 1d. However, NBO analysis suggested this dimer is not held together by HBs, but rather by a tetrel bond wherein the O lone pairs transfer charge into the σ*(CS) antibonding orbital. This transfer, amounting to 2.59 kcal/mol, is aided by the close approach of the O and C atoms, 2.694 Å, and the near linearity of the O··CS triad. However, this tetrel bond represents the weakest of the interactions of the NMA/$S(CH_3)_3^+$ pair, bound by only 13.72 kcal/mol. It may be noted finally that the results summarized in Fig 1 are consistent with a recent set of calculations [87], quantitatively as well as qualitatively, at a different level of theory.

$SH_2CH_3^+$

The removal of two of the methyl groups, replacing them by H atoms, permits the elucidation of a O··S-C chalcogen bond free of the CH··O HBs of Fig 1a. The $SH_2CH_3^+$ cation, however, contains a powerful proton donor SH group that rotates this cation around so that one SH bond is facing the O atom of NMA. Indeed, the cationic SH is a strong enough proton donor that the bridging proton transfers across to the NMA, leaving a OH^+···S HB. In order to prevent this transfer, the r(SH) bond length was held to 1.36 Å, the same length as in the optimized $SH_2CH_3^+$ monomer. The resulting SH··O H-bonding complex is bound by 29.24 kcal/mol, as indicated in Fig 2a. HBs tend to have particularly large charge transfer energies, and this geometry is no exception, with E(2) greater than 70 kcal/mol.

The O··SC chalcogen bonded structure is also quite stable, bound by 21.95 kcal/mol. Again due to the tendency of the $SH_2CH_3^+$ cation to rotate so as to present its SH_2 group to the NMA, this structure was optimized with the restraint that θ(O··SC)=180°. The geometry in Fig 2b is bound by 21.95 kcal/mol, largely due to the charge transfer from the O lone pairs into the σ*(SC) antibonding orbital, amounting to 5.66 kcal/mol. The SH protons are within striking distance of the NMA O atom, both around 2.6 Å, but the θ(SH··O) angles are so far from linearity that there is no significant charge transfer into the σ*(SH) orbitals, so any SH··O HB is extremely weak, and the full interaction can be ascribed to the O··SC chalcogen bond.

The methyl end of the $SH_2CH_3^+$ cation can also engage in an attractive interaction with the NMA. A structure of this sort is illustrated in Fig 2c, which was optimized with no geometrical restraints. As in the case of $S(CH_3)_3^+$ this complex is bound by a tetrel bond, with E(2) for $O_{lp}\rightarrow\sigma^*CS$ transfer equal to 3.72 kcal/mol. (There is no significant $O_{lp}\rightarrow\sigma^*CH$ transfer.) A single CH··O H-bonding arrangement does not correspond to a minimum on the potential energy surface, but was generated by restraining a θ(CH··O) angle to 180°. The optimized structure, bound by 18.33 kcal/mol, is illustrated in Fig 2d. It contains a linear CH··O HB with R(O··H)=1.857 Å, with a large charge transfer energy E(2) of 14.45 kcal/mol. Note that this single linear CH··O HB is somewhat more stable than the tetrel bonded structure 2c. But both are exceeded by the O··SC chalcogen bond.

$SHCH_3$

Both $S(CH_3)_3^+$ and $SH_2CH_3^+$ are positively charged, and thus have amplified interactions. The removal of a proton from the latter to form $SHCH_3$ ought to yield weaker binding with NMA. Even so, this neutral molecule can still engage in a fairly strong SH··O HB, with a binding energy of 4.12 kcal/mol, as displayed in Fig 3a. There are no CH··S bonds present in this structure, as evident by no significant charge transfers, and with long H··S distances of 3.23 Å. Another minimum corresponds to a

tetrel bond 3b. The $O_{lp}\rightarrow\sigma^*CS$ charge transfer is less than 1 kcal/mol, but sufficient to provide a binding energy of 1.90 kcal/mol. A single CH··O H-bonded configuration is only secured after restricting the θ(CH··O) angle to 180°, and is slightly less stable, bound by 1.67 kcal/mol. (Structure 3c requires a second restriction, that an internal φ(HSCH) dihedral angle be held at 0°, to prevent the formation of a CH··S HB.) The standard $O_{lp}\rightarrow\sigma^*CH$ charge transfer of 2.85 kcal/mol is supplemented by 1.39 kcal/mol derived from transfer from the CO π bonding orbital. The chalcogen bond in this dimer is quite weak, with structure 3d bound by only 1.14 kcal/mol. Moreover, this geometry is not a true minimum, and is obtained only when θ(O··SC) is held at 180°. E(2) for the $O_{lp}\rightarrow\sigma^*SC$ charge transfer is less than 1 kcal/mol. Removal of the charge from the S-containing unit thus weakens all interactions, but especially the chalcogen bond.

$\underline{FHSCH_3^+}$

In addition to adding a positive charge to the entire unit, the electron-accepting ability of a given molecule can also be enhanced by substitution of a H atom by the strongly electron-withdrawing F. The combined effect of these two modifications were studied by consideration of $FHSCH_3^+$. When combined with NMA, the most stable configuration of the resulting dimer contains the O··SF chalcogen bond, pictured in Fig 4a. This complex is bound by a full 39 kcal/mol, and owes its stability in large measure to the $O_{lp}\rightarrow\sigma^*SF$ charge transfer of 96.6 kcal/mol. Another sort of chalcogen bond places the methyl group opposite the NMA O atom. However, this structure 4b is not a true minimum, and can only be obtained by fixing θ(O··SC)=180°. Nonetheless, it is bound rather strongly, by 23.43 kcal/mol. The standard $O_{lp}\rightarrow\sigma^*SC$ charge transfer of 5.87 kcal/mol is supplemented by an additional 1.71 kcal/mol resulting from transfer into the σ*SF antibonding orbital. As in the earlier case of a cation, a full optimization will result in the transfer of a proton from S to the NMA molecule. The SH··O H-bonding structure 4c was thus obtained by again freezing r(SH) at 1.36 Å to prevent this transfer. The SH··O HB is quite strong, with a huge E(2) of nearly 100 kcal/mol, but is nonetheless overshadowed by the O··SF chalcogen bond in 4a. A CH··O HB is also feasible, but requires the restriction of a θ(CH··O) angle of 180° to obtain such a structure. Configuration 4d reflects a binding energy of 21.17 kcal/mol, nearly as strong as the O··SC chalcogen bond of 4b. Direct approach of the NMA O atom toward the C atom leads to the tetrel-bonded structure 4e. This geometry is slightly less stable than the CH··O HB configuration of 4d. Like 4d, 4e also requires a geometrical restriction, in this case θ(O··CS)=180°.

$\underline{SFCH_3}$

As before, the positive charge of the fluorosubstituted $FHSCH_3^+$ was removed by virtue of the neutral $FSCH_3$ molecule. As in the case of the cation, the most stable minimum again contains a O··SF chalcogen bond. Structure 5a is bound by 6.40 kcal/mol and the $O_{lp}\rightarrow\sigma^*SF$ charge transfer amounts to 3.55 kcal/mol. There is a small supplement from a weak CH··O HB: although r(H··O) is only 2.34 Å, θ(CH··O) is 64° removed from linearity. The other chalcogen bond, O··SC, also represents a minimum on the surface, but, is considerably weaker with a binding energy of 2.71 kcal/mol. In addition to the expected $O_{lp}\rightarrow\sigma^*SC$ charge transfer, there are also contributions from a CH··S HB $S_{lp}\rightarrow\sigma^*(CH)$ and $F_{lp}\rightarrow\pi^*(CO)$ back transfer. The CH··O configuration 5c is bound by 3.29, making this HB stronger than the O··SC chalcogen bond. Somewhat weaker is the tetrel bond 5d, amounting to 2.50 kcal/mol.

AIM analysis

In addition to assessing the charge transfer between individual orbitals of the interaction molecules as a means of determining the presence of noncovalent bonds, analysis of the electron density via the

AIM procedure is another means of identifying such bonds. The intermolecular bond critical points (BCPs) were located and their densities, and density Laplacians, are reported in Tables 3 and 4, respectively. Comparison with the charge transfers in Table 2 confirm many of the NBO conclusions. Taking the first entries in the Tables as an example, both NBO and AIM suggest that the O··S chalcogen bond between the NMA O atom and the S of $S(CH_3)_3^+$ is supplemented by a pair of CH··O HBs, of perhaps comparable strength. The linear CH··O structure of this same pair also combines a much weaker CH··O from a second methyl group. NBO and AIM agree that the strongest interactions are associated with the cationic electron acceptors, particularly for the O··SF alignment. Both methods also seem to exaggerate the strengths of HBs when compared with other noncovalent bonds, in that E(2), ρ_{BCP}, and $\nabla^2\rho_{BCP}$ are all larger than would be expected on the basis of the binding energies, although E(2) is perhaps guiltier in this regard.

There are also some significant differences between the NBO and AIM results. For example, AIM suggests a bond, albeit a weak one, between a pair of methyl H atoms in the CH··O configuration of CH_3SH, 3c, whereas NBO contains no such indication. The two means of analysis differ appreciably in the context of the O··SC configuration of $FSCH_3$, 5b. In the first place, the NBO picture takes the origin of the charge into the σ*SC antibond as the πCO bond of NMA, rather than the usual O lone pairs. This interaction is supplemented by a CH··S HB and transfer from F lone pairs into the π*CO antibonding orbital. The CH··S HB is confirmed by AIM, and the latter transfer emerges as a F··C bond. But AIM also adds a CH··F HB to the mix, a bond which is not indicated by NBO.

Coulombic Interactions

The molecular electrostatic potential (MEP) around a given molecule is typically a key factor in its interactions with another monomer. The MEPs of the systems under consideration are presented in Fig 6. In the case of the cations, this potential is positive everywhere, so the diagrams vary from most to least positive regions; the two neutral systems illustrate both positive and negative areas. Since the binding involves interaction with the negative region surrounding the O atom of NMA, the MEPs ought to guide the O toward the most positive, i.e. bluest, areas of the electron acceptor molecules. This model is at least partially successful. First considering $S(CH_3)_3^+$, there are strongly blue areas in the "seams" between the H atoms, which can account for the global minimum with its trifurcated CH··O HB, as well as the O··SC structure. On the other hand, the region that would lead to the tetrel bond is considerably less positive. Nor is there a blue region that would correspond to a tetrel bond for $H_2SCH_3^+$, and the same is true of the extension of the C-S bond that would be associated with a O··SC chalcogen bond. The MEP is perhaps more useful for $FHSCH_3^+$, where the most positive regions correspond to the SH··O and O··SF configurations, the two most strongly bound complexes. The potential surrounding $HSCH_3$ would suggest both SH··O and CH··O HBs. Whereas the former is correct, it is in fact the tetrel bond that is stronger than CH··O; the chalcogen bond is not a minimum on this surface. Lastly, on the basis of its MEP, $FSCH_3$ might be expected to have both a O··SF and CH··O minimum. The former is a correct prediction, but neither a HB nor a tetrel bond represent minima. The O··SC chalcogen-bonded true minimum would probably not be guessed from simple examination of the MEP of $FSCH_3$. In summary, study of the MEP is useful here, but cannot be relied on to provide accurate predictions in all cases.

Perturbations of Monomers

The formation of noncovalent bonds usually induces changes into the internal geometries of the participating monomers, which can be helpful in understanding the fundamental aspects of the

interaction. The perturbations of the key bonds in each interaction are displayed in Table 5 where the bond of interest is indicated by the double arrow. Clearly, the largest changes are undergone by the strong S-F bond in the O···SF chalcogen bonds. These large bond elongations are largely a result of the strong charge transfer into the σ*(SF) antibonding orbital. A similar, albeit smaller, charge is transferred into the σ*(SC) bonds in the O··SC configurations in the first column of Table 3, so the bond elongations are smaller. Note that there is no true minimum associated with the O··SC configuration of $CH_3SH_2^+$, which may have something to do with the failure of the S-C bond to elongate, and in fact to contract. This contraction may also be associated with a 1.8% increase in the s-character, and associated decrease in p-character, in the hybridization of the C atom within the C-S bonding orbital, via Bent's rule [88]. Transfer into the σ*(CS) antibond leads to an elongation of the corresponding covalent bond in the tetrel interactions, with the exception of the weak intermolecular interaction of $FSCH_3$. The CH bonds elongate when engaging in a CH··O HB, particularly in the very strong bond with $FHSCH_3^+$. There is a general correlation between E(2) and Δr for these bonds.

NMR has proven to be an extremely useful tool in deciphering the structure of numerous molecular complexes over the years. In particular, H-bonding protons typically undergo a notable downfield shift of their chemical shift in comparison to the uncomplexed molecule. In order to facilitate NMR analysis of the various complexes examined here, the isotropic chemical shifts have been computed and related to the uncomplexed monomer. The changes induced by complexation are compiled in Table 6 for the methyl protons. Since the methyl rotations are generally too fast to pull out the signals of individual protons, the average change of the three methyl protons are reported in the table. In those cases where the H atom participates in a HB, its change is reported separately, in addition to the average of all three.

In those cases where a CH group of methyl engages directly in a CH··O HB, its signal clearly shifts downfield. This amount varies from a minimum of 1.1 ppm for the weak HB formed by neutral CH_3SH to as much as 5.2 ppm in the stronger proton donor $FHSCH_3^+$. Indeed, the amount of the shift is roughly proportional to the binding energy reported in Table 1. The large downfield shift of this proton overwhelms the upfield shift of the other two protons on the pertinent methyl group, leaving the average of the three as a small negative quantity. The latter is slightly more negative than the downfield shift of the three protons when the methyl group is engaged in a tetrel bond with the NMA O atom, which is sometimes (incorrectly) described as a trifurcated HB. Consequently, if the time scale of the methyl rotation permits the identification of the H-bonding proton from the other two methyl hydrogens, it would be straightforward to distinguish a CH··O configuration from a tetrel bond, but much more difficult to do so if the methyl rotation is fast.

Both of these situations are easily differentiated from the other types of bonding situations. In the case of O··SC chalcogen bonds, which do not involve the methyl group directly, the protons of the latter undergo a small upfield shift, less than 0.6 ppm. The shift is smaller for the O··SF configurations only because one methyl H atom participates in a weak CH··O HB, and is thus shifted downfield by a small amount. Participation of a charged species in a SH··O HB yields a small upfield shift of the methyl protons, difficult to distinguish from a like shift occurring for a O··SC chalcogen bond; no methyl shift occurs for a neutral molecule.

SUMMARY AND DISCUSSION

There are a number of ways in which a methyl-substituted S-compound can interact with an electron donor. In the first place, the methyl groups can participate in CH··O HBs which are more or less linear arrangements. The electron donor O atom can also approach the C atom of the methyl group directly, along a line between the three H atoms, in what has come to be called a tetrel bond. A chalcogen bond is formed as a result of interaction with the S atom, usually along a line directly opposite one of the S-C or S-X covalent bonds. A last alternative is the formation of a SH··O HB.

Calculations suggest that the strengths of these interactions are generally competitive with one another. But there are perhaps useful overarching rules that can be elucidated. In the first place, a cation engages in much stronger noncovalent bonds than do the neutrals. This result is sensible, and comports with prior results [50, 89-90]. More specifically, the binding energies for the neutrals cover the range between 1 and 6 kcal/mol, whereas the positively charged acceptors bind with strengths varying between 14 and 39 kcal/mol. The strongest noncovalent bond for any system is a O··SF chalcogen bond wherein the O lies directly opposite a S-F covalent bond if one is present. Second in binding energy is the SH··O HB. The other three interactions are somewhat weaker, and competitive with one another. In the context of the charged systems, these noncovalent bonds obey the pattern O··SC > CH··O > O··C, where the latter refers to the tetrel bond. Pursuant to the $(CH_3)_3S^+$ results, a O··SC chalcogen bonding arrangement is competitive with a trifurcated H-bond, involving three different alkyl groups. When the molecule does not bear a positive charge, chalcogen, CH··O and O··C tetrel bonds are close in energy: The tetrel bond is strongest of the three for CH_3SH while the CH··O HB has the largest binding energy for $FSCH_3$.

In a strict sense, not all of these interactions represent true minima on the potential energy surface. Some of them were obtained only after a suitable geometric restraint was placed on the system. The CH··O H-bonding structure is a case in point where a linear configuration was imposed. The O··SC structure was another bond which was acquired only after a linear arrangement was imposed, at least for certain dimers. Because the O atom of NMA is a stronger base than is the S of cationic species, a full optimization of the SH··O dimer leads to the transfer of the proton from S to O. This transfer was avoided by freezing the r(SH) distance during optimizations of the SH··O configurations. Even if not a true minimum, the evaluation of the binding energy and its contributing factors represents an important issue when these groups are placed within the context of larger systems such as proteins, where full optimization would be precluded by geometrical restraints imposed by the macromolecular system.

NBO and AIM analysis of the various geometries facilitates an elucidation of the fundamental properties of each interaction. Both methods agree, for example, that in the tetrel-bonding geometries, the interaction arises exclusively between the O and C atoms, with no evidence of any CH··O HBs even though there are three methyl H atoms in proximity to the approaching oxygen. In some cases, the primary noncovalent bond is supplemented by secondary, albeit weaker, interactions. The O···SC chalcogen bonding structure of $(CH_3)_3S^+$, for example, also contains elements of a pair of weaker CH··O HBs. This same O···SC geometry of neutral $FSCH_3$ is aided not only by a CH··S HB but also by an attractive F··C interaction.

While NBO and AIM are in general agreement as to these augmenting interactions, there are a number of cases of disagreement as well. The CH··O H-bonding structure of CH_3SH is a case in point, where AIM analysis suggests a CH··HC bond between a pair of H atoms, whereas no such interaction

arises in the NBO treatment, which provides instead for a OC→σ*CH transfer. Disagreements such as these are not uncommon in the literature [91-98] as the two methods are quite different in terms of formulation. In quantitative terms, the NBO charge transfer parameter E(2) and the AIM bond critical point properties are roughly proportional to the binding energy. On the other hand, both procedures seem to provide systematically larger indicators of the strengths of HBs in comparison to chalcogen and tetrel bonds of equal energy.

One is now in a position to address the question as to preferred site of binding, and cost of disrupting a particular interaction. It should first be stressed that a methyl group can interact via either a CH··O HB or a C··O tetrel bond. Since these interactions have comparable binding energies, it is apparent that a methyl group presents a broad area for binding. Distortion of a direct O··C approach toward one of the H atoms does not represent a substantial loss of binding energy. So ensuing discussion will bring both of these interactions under the umbrella of what might be termed a "methyl" interaction. Chalcogen and SH··O HBs on the other hand, will be more sensitive to angular distortion, so should be considered in this light.

In the case of a neutral molecule, binding energies are rather small, in the 2-4 kcal/mol range. The only binding that exceeds even 2 kcal/mol is a SH··O HB, more than double that involving either methyl or chalcogen bonds. Substitution of a strongly electron withdrawing substituent on the S atom, e.g. F, will enhance all of the interactions, bringing them up to the 3-6 kcal/mol range; the strongest of these is a O··SF chalcogen bond. There will be little to distinguish a O··SC chalcogen from a methyl interaction. The situation changes when positive charge is added to the electron acceptor, and all bonds are magnified in strength up to the 16-29 kcal/mol range. A SH··O HB is the strongest noncovalent bond, but a chalcogen bond is favored over an interaction with a methyl group. In the case of a trialkylated sulfonium such as $(CH_3)_3S^+$, where there is no SH group or possible SH··O, the chalcogen bond is quite strong, preferred over a methyl interaction by several kcal/mol. On the other hand, if geometrical restrictions permit the oncoming electron donor to interact with several alkyl groups simultaneously, the presence of multiple CH··O HBs can effectively compete with the chalcogen bond. Addition of an electronegative substituent like F leads to the strongest bond of any in this study, viz. a O··SF chalcogen bond, which approaches 40 kcal/mol. Even the weaker O··SC chalcogen bond accounts for as much as 23 kcal/mol, and is preferred over interaction with the methyl group by some 2-6 kcal/mol.

It should be stressed that certain arrangements of the pair of species can be characterized as stabilized by more than one sort of bond. As an example, chalcogen-bonded O··SC arrangement 1a of $(CH_3)_3S^+$ contains CH··O HB elements as well. Such multiple interactions would be even more common in a biological context where forces external to the molecular pair of interest might restrain them from assuming a structure consistent with a pure chalcogen, or H-bond. The bonding in such situations would then be best described by several bonds, each of which is strained and thereby weakened. In the context of the methyl transferase family of enzymes, there would be a major functional difference between a tetrel bond and a CH··O HB, since the former may serve as a precursor to the S_N2 methyl transfer reaction [77-80].

NMR has potential as a diagnostic tool by which to distinguish one sort of bonding from another. Any CH group which participates in a CH··O HB shifts downfield by an amount which is roughly proportional to the strength of the HB. This shift can be as large as 5 ppm, and would mark its presence even if the methyl rotation were too rapid to distinguish the three proton signals from one another. The

shift of the CH··O bridging proton far exceeds the much smaller downfield shift, less than 1 ppm, of the methyl protons when engaged in a trifurcated structure, i.e. a tetrel bond. In contrast, formation of a O··S chalcogen or SH··O HB would tend to shift the protons of the non-participating methyl group upfield, clearly distinguishable from the former CH··O or O··C geometries.\

ACKNOWLEDGMENTS

I am grateful to Prof. Raymond Trievel for a careful reading of this manuscript.

REFERENCES

1. Joesten, M. D.; Schaad, L. J. *Hydrogen Bonding*. Marcel Dekker: New York, 1974; p 622.
2. Schuster, P.; Zundel, G.; Sandorfy, C. *The Hydrogen Bond. Recent Developments in Theory and Experiments*. North-Holland Publishing Co.: Amsterdam, 1976.
3. Schuster, P. *Hydrogen Bonds*. Springer-Verlag: Berlin, 1984; Vol. 120, p 117.
4. Arunan, E.; Desiraju, G. R.; Klein, R. A.; Sadlej, J.; Scheiner, S.; Alkorta, I.; Clary, D. C.; Crabtree, R. H.; Dannenberg, J. J.; Hobza, P., et al. Definition of the Hydrogen Bond. *Pure Appl. Chem.* **2011,** *83*, 1637-1641.
5. Jablonski, M.; Sokalski, W. A. Physical Nature of Interactions in Charge-Inverted Hydrogen Bonds. *Chem. Phys. Lett.* **2012,** *552*, 156-161.
6. Falvello, L. R. The Hydrogen Bond, Front and Center. *Angew. Chem., Int. Ed. Engl.* **2010,** *49*, 10045-10047.
7. Latajka, Z.; Scheiner, S. Structure, Energetics and Vibrational Spectrum of H_2O-HCl. *J. Chem. Phys.* **1987,** *87*, 5928-5936.
8. Sandoval-Lira, J.; Fuentes, L.; Quintero, L.; Höpfl, H.; Hernández-Pérez, J. M.; Terán, J. L.; Sartillo-Piscil, F. The Stabilizing Role of the Intramolecular C–H···O Hydrogen Bond in Cyclic Amides Derived from A-Methylbenzylamine. *J. Org. Chem.* **2015,** *80*, 4481-4490.
9. Adhikari, U.; Scheiner, S. Competition between Lone Pair–Π, Halogen Bond, and Hydrogen Bond in Adducts of Water with Perhalogenated Alkenes $C_2Cl_nF_{4-n}$ (n=0–4). *Chem. Phys.* **2014,** *440*, 53-63.
10. Hansen, A. S.; Du, L.; Kjaergaard, H. G. Positively Charged Phosphorus as a Hydrogen Bond Acceptor. *J. Phys. Chem. Lett.* **2014,** *5*, 4225-4231.
11. Latajka, Z.; Scheiner, S. Basis Sets for Molecular Interactions. 2. Application to H_3N-HF, H_3N-HOH, H_2O-HF, $(NH_3)_2$, and H_3CH-OH_2. *J. Comput. Chem.* **1987,** *5*, 674-682.
12. Joseph, R.; Nkrumah, A.; Clark, R. J.; Masson, E. Stabilization of Cucurbituril/Guest Assemblies Via Long-Range Coulombic and CH···O Interactions. *J. Am. Chem. Soc.* **2014,** *136*, 6602-6607.
13. Orlova, G.; Scheiner, S. Intermolecular MH···HF Bonding in Monohydride Mo and W Complexes. *J. Phys. Chem. A* **1998,** *102*, 260-269.
14. Grabowski, S. J. Dihydrogen Bond and X-H···σ Interaction as Sub-Classes of Hydrogen Bond. *J. Phys. Org. Chem.* **2013,** *26*, 452-459.
15. Latajka, Z.; Scheiner, S. Structure, Energetics and Vibrational Spectra of Dimers, Trimers, and Tetramers of HX (X = Cl, Br, I). *Chem. Phys.* **1997,** *216*, 37-52.
16. Mundlapati, V. R.; Ghosh, S.; Bhattacherjee, A.; Tiwari, P.; Biswal, H. S. Critical Assessment of the Strength of Hydrogen Bonds between the Sulfur Atom of Methionine/Cysteine and Backbone Amides in Proteins. *J. Phys. Chem. Lett.* **2015,** *6*, 1385-1389.
17. Scheiner, S. Detailed Comparison of the Pnicogen Bond with Chalcogen, Halogen and Hydrogen Bonds. *Int. J. Quantum Chem.* **2013,** *113*, 1609-1620.
18. Biswal, H. S.; Wategaonkar, S. Sulfur, Not Too Far Behind O, N, and C: SH···π Hydrogen Bond. *J. Phys. Chem. A* **2009,** *113*, 12774-12782.
19. Cabaleiro-Lago, E. M.; Rodríguez-Otero, J.; Peña-Gallego, Á. Characteristics of the Interaction of Azulene with Water and Hydrogen Sulfide: A Computational Study. *J. Chem. Phys.* **2008,** *129*, 084305.
20. Bhattacherjee, A.; Matsuda, Y.; Fujii, A.; Wategaonkar, S. Acid–Base Formalism in Dispersion-Stabilized S–H···Y (Y═O, S) Hydrogen-Bonding Interactions. *J. Phys. Chem. A* **2015,** *119*, 1117-1126.
21. Solimannejad, M.; Gharabaghi, M.; Scheiner, S. SH···N and SH···P Blue-Shifting H-Bonds and N···P Interactions in Complexes Pairing Hsn with Amines and Phosphines. *J. Chem. Phys.* **2011,** *134*, 024312.

22. Minkov, V. S.; Boldyreva, E. V. Contribution of Weak S–H···O Hydrogen Bonds to the Side Chain Motions in D,L-Homocysteine on Cooling. *J. Phys. Chem. B* **2014,** *118*, 8513-8523.
23. Biswal, H. S. Hydrogen Bonds Involving Sulfur: New Insights from Ab Initio Calculations and Gas Phase Laser Spectroscopy. In *Noncovalent Forces*, Scheiner, S., Ed. Springer: Dordrecht, 2015; Vol. 19, pp 15-45.
24. Cybulski, S.; Scheiner, S. Hydrogen Bonding and Proton Transfers Involving Triply Bonded Atoms. HC≡N and HC≡CH. *J. Am. Chem. Soc.* **1987,** *109*, 4199-4206.
25. Zierke, M.; Smieško, M.; Rabbani, S.; Aeschbacher, T.; Cutting, B.; Allain, F. H.-T.; Schubert, M.; Ernst, B. Stabilization of Branched Oligosaccharides: Lewis Benefits from a Nonconventional C–H···O Hydrogen Bond. *J. Am. Chem. Soc.* **2013,** *135*, 13464-13472.
26. Gu, Y.; Kar, T.; Scheiner, S. Comparison of the CH···N and CH···O Interactions Involving Substituted Alkanes. *J. Mol. Struct.* **2000,** *552*, 17-31.
27. Michielsen, B.; Verlackt, C.; van der Veken, B. J.; Herrebout, W. A. C–H···X (X = S, P) Hydrogen Bonding: The Complexes of Halothane with Dimethyl Sulfide and Trimethylphosphine. *J. Mol. Struct.* **2012,** *1023*, 90-95.
28. Scheiner, S.; Kar, T. Effect of Solvent Upon CH··O Hydrogen Bonds with Implications for Protein Folding. *J. Phys. Chem. B* **2005,** *109*, 3681-3689.
29. Sánchez-Sanz, G.; Trujillo, C.; Alkorta, I.; Elguero, J. Weak Interactions between Hypohalous Acids and Dimethylchalcogens. *Phys. Chem. Chem. Phys.* **2012,** *14*, 9880-9889.
30. Kryachko, E.; Scheiner, S. CH··F Hydrogen Bonds. Dimers of Fluoromethanes. *J. Phys. Chem. A* **2004,** *108*, 2527-2535.
31. Christenholz, C. L.; Obenchain, D. A.; Peebles, R. A.; Peebles, S. A. Rotational Spectroscopic Studies of C–H···F Interactions in the Vinyl Fluoride···Difluoromethane Complex. *J. Phys. Chem. A* **2014,** *118*, 1610-1616.
32. Solimannejad, M.; Malekani, M.; Alkorta, I. Cooperativity between the Hydrogen Bonding and Halogen Bonding in F_3CX ··· NCH(CNH) ··· NCH(CNH) Complexes (X=Cl, Br). *Mol. Phys.* **2011,** *109*, 1641-1648.
33. Scheiner, S. Relative Strengths of NH··O and CH··O Hydrogen Bonds between Polypeptide Chain Segments. *J. Phys. Chem. B* **2005,** *109*, 16132-16141.
34. Jones, C. R.; Baruah, P. K.; Thompson, A. L.; Scheiner, S.; Smith, M. D. Can a C-H···O Interaction Be a Determinant of Conformation. *J. Am. Chem. Soc.* **2012,** *134*, 12064-12071.
35. Beyeh, N. K.; Pan, F.; Rissanen, K. A Halogen-Bonded Dimeric Resorcinarene Capsule. *Angew. Chem. Int. Ed.* **2015,** *54*, 7303-7307.
36. Zheng, Q.-N.; Liu, X.-H.; Chen, T.; Yan, H.-J.; Cook, T.; Wang, D.; Stang, P. J.; Wan, L.-J. Formation of Halogen Bond-Based 2d Supramolecular Assemblies by Electric Manipulation. *J. Am. Chem. Soc.* **2015,** *137*, 6128-6131.
37. Politzer, P.; Murray, J. S. A Unified View of Halogen Bonding, Hydrogen Bonding and Other σ-Hole Interactions. In *Noncovalent Forces*, Scheiner, S., Ed. Springer: Dordrecht, 2015; Vol. 19, pp 357-389.
38. Adhikari, U.; Scheiner, S. Substituent Effects on Cl···N, S···N, and P···N Noncovalent Bonds. *J. Phys. Chem. A* **2012,** *116*, 3487-3497.
39. Zierkiewicz, W.; Bieńko, D. C.; Michalska, D.; Zeegers-Huyskens, T. Theoretical Investigation of the Halogen Bonded Complexes between Carbonyl Bases and Molecular Chlorine. *J. Comput. Chem.* **2015,** *36*, 821-832.
40. Joseph, J. A.; McDowell, S. A. C. Comparative Computational Study of Model Halogen-Bonded Complexes of FKrCl. *J. Phys. Chem. A* **2015,** *119*, 2568-2577.

41. Riley, K. E.; Ford Jr, C. L.; Demouchet, K. Comparison of Hydrogen Bonds, Halogen Bonds, CH···p Interactions, and CX···π Interactions Using High-Level Ab Initio Methods. *Chem. Phys. Lett.* **2015,** *621*, 165-170.
42. Robinson, S. W.; Mustoe, C. L.; White, N. G.; Brown, A.; Thompson, A. L.; Kennepohl, P.; Beer, P. D. Evidence for Halogen Bond Covalency in Acyclic and Interlocked Halogen-Bonding Receptor Anion Recognition. *J. Am. Chem. Soc.* **2015,** *137*, 499-507.
43. McDowell, S. A. C.; Joseph, J. A. A Comparative Study of Model Halogen-Bonded, π-Hole-Bonded and Cationic Complexes Involving NCX and H_2O (X = F, Cl, Br). *Mol. Phys.* **2015,** *113*, 16-21.
44. Grabowski, S. J. Halogen Bond with the Multivalent Halogen Acting as the Lewis Acid Center. *Chem. Phys. Lett.* **2014,** *605-606*, 131-136.
45. Hauchecorne, D.; Herrebout, W. A. Experimental Characterization of C–X···Y–C (X = Br, I; Y = F, Cl) Halogen–Halogen Bonds. *J. Phys. Chem. A* **2013,** *117*, 11548-11557.
46. Adhikari, U.; Scheiner, S. Sensitivity of Pnicogen, Chalcogen, Halogen and H-Bonds to Angular Distortions. *Chem. Phys. Lett.* **2012,** *532*, 31-35.
47. Bauzá, A.; Quiñonero, D.; Deyà, P. M.; Frontera, A. Halogen Bonding Versus Chalcogen and Pnicogen Bonding: A Combined Cambridge Structural Database and Theoretical Study. *CrystEngComm* **2013,** *15*, 3137-3144.
48. Bauzá, A.; Mooibroek, T. J.; Frontera, A. The Bright Future of Unconventional σ/π-Hole Interactions. *ChemPhysChem.* **2015**, DOI: 10.1002/cphc.201500314.
49. Rosenfield, R. E.; Parthasarathy, R.; Dunitz, J. D. Directional Preferences of Nonbonded Atomic Contacts with Divalent Sulfur. 1. Electrophiles and Nucleophiles. *J. Am. Chem. Soc.* **1977,** *99*, 4860-4862.
50. Adhikari, U.; Scheiner, S. Effects of Charge and Substituent on the S···N Chalcogen Bond. *J. Phys. Chem. A* **2014,** *118*, 3183-3192.
51. Pang, X.; Jin, W. J. Exploring the Halogen Bond Specific Solvent Effects in Halogenated Solvent Systems by Esr Probe. *New J. Chem.* **2015,** *39*, 5477-5483.
52. Azofra, L. M.; Alkorta, I.; Scheiner, S. Chalcogen Bonds in Complexes of Soxy (X, Y = F, Cl) with Nitrogen Bases. *J. Phys. Chem. A* **2015,** *119*, 535-541.
53. Si, M. K.; Lo, R.; Ganguly, B. The Origin and Magnitude of Intramolecular Quasi-Cyclic S···O and S···S Interactions Revisited: A Computational Study. *Chem. Phys. Lett.* **2015,** *631–632*, 6-11.
54. Esrafili, M.; Mohammadian-Sabet, F. Ab Initio Calculations of Cooperativity Effects on Chalcogen Bonding: Linear Clusters of $(OCS)_{2–8}$ and $(OCSe)_{2–8}$. *Struct. Chem.* **2015,** *26*, 199-206.
55. Nziko, V. d. P. N.; Scheiner, S. Intramolecular S···O Chalcogen Bond as Stabilizing Factor in Geometry of Substituted Phenyl-SF_3 Molecules. *J. Org. Chem.* **2015,** *80*, 2356-2363.
56. Scheiner, S. Effects of Multiple Substitution Upon the P···N Noncovalent Interaction. *Chem. Phys.* **2011,** *387*, 79-84.
57. Del Bene, J. E.; Alkorta, I.; Elguero, J. Properties of Cationic Pnicogen-Bonded Complexes $F_{4–n}H_nP^+$:N-Base with F–P···N Linear and n = 0–3. *J. Phys. Chem. A* **2015,** *119*, 5853-5864.
58. Del Bene, J. E.; Alkorta, I.; Elguero, J. The Pnicogen Bond in Review: Structures, Energies, Bonding Properties, and Spin-Spin Coupling Constants of Complexes Stabilized by Pnicogen Bonds. In *Noncovalent Forces*, Scheiner, S., Ed. Springer: Dordrecht, 2015; Vol. 19, pp 191-263.
59. Scheiner, S. On the Properties of X···N Noncovalent Interactions for First-, Second- and Third-Row X Atoms. *J. Chem. Phys.* **2011,** *134*, 164313.
60. Sarkar, S.; Pavan, M. S.; Guru Row, T. N. Experimental Validation of 'Pnicogen Bonding' in Nitrogen by Charge Density Analysis. *Phys. Chem. Chem. Phys.* **2015,** *17*, 2330-2334.
61. Latajka, Z.; Scheiner, S. Effects of Basis Set and Electron Correlation on the Calculated Properties of the Ammonia Dimer. *J. Chem. Phys.* **1984,** *81*, 407-409.

62. Oliveira, B. G. Theoretical Estimation of Pnicogen Bonds and Hydrogen Bonds in Small Heterocyclic Complexes: Red-Shifts and Blue-Shifts Ruled by Polarization Effects. *Chem. Phys.* **2014,** *443*, 67-75.
63. Mani, D.; Arunan, E. The X–C⋯π (X = F, Cl, Br, CN) Carbon Bond. *J. Phys. Chem. A* **2014,** *118*, 10081-10089.
64. Tang, Q.; Li, Q. Interplay between Tetrel Bonding and Hydrogen Bonding Interactions in Complexes Involving F_2xo (X=C and Si) and HCN. *Comput. Theor. Chem.* **2014,** *1050*, 51-57.
65. Vijaya Pandiyan, B.; Deepa, P.; Kolandaivel, P. On the Nature of Non-Covalent Interactions in Isomers of 2,5-Dichloro-1,4-Benzoquinone Dimers - Ground- and Excited-State Properties. *Phys. Chem. Chem. Phys.* **2014,** *16*, 19928-19940.
66. McDowell, S. A. C. Sigma-Hole Cooperativity in Anionic $[FX\cdots CH_3\cdots YF]^-$ (X, Y = Cl, Br) Complexes. *Chem. Phys. Lett.* **2014,** *598*, 1-4.
67. Alkorta, I.; Elguero, J.; Solimannejad, M. Single Electron Pnicogen Bonded Complexes. *J. Phys. Chem. A* **2014,** *118*, 947-953.
68. Grabowski, S. J. Tetrel Bond–σ-Hole Bond as a Preliminary Stage of the S_n2 Reaction. *Phys. Chem. Chem. Phys.* **2014,** *16*, 1824-1834.
69. Bauzá, A.; Mooibroek, T. J.; Frontera, A. Tetrel-Bonding Interaction: Rediscovered Supramolecular Force? *Angew. Chem. Int. Ed.* **2013,** *52*, 12317-12321.
70. Azofra, L. M.; Scheiner, S. Tetrel, Chalcogen, and CH⋯O Hydrogen Bonds in Complexes Pairing Carbonyl-Containing Molecules with 1, 2, and 3 Molecules of CO_2. *J. Chem. Phys.* **2015,** *142*, 034307.
71. Krimm, S. Hydrogen Bonding of C - H • • • O = C in Proteins. *Science* **1967,** *158*, 530-531.
72. Ramachandran, G. N.; Chandrasekharan, R. Interchain Hydrogen Bonds Via Bound Water Molecules in the Collagen Triple Helix. *Biopolymers* **1968,** *6*, 1649-1658.
73. Derewenda, Z. S.; Lee, L.; Derewenda, U. The Occurrence of C-H⋯O Hydrogen Bonds in Proteins. *J. Mol. Biol.* **1995,** *252*, 248-262.
74. Musah, R. A.; Jensen, G. M.; Rosenfeld, R. J.; McRee, D. E.; Goodin, D. B.; Bunte, S. W. Variation in Strength of an Unconventional C-H to O Hydrogen Bond in an Engineered Protein Cavity. *J. Am. Chem. Soc.* **1997,** *119*, 9083-9084.
75. Lee, K. M.; Chang, H.-C.; Jiang, J.-C.; Chen, J. C. C.; Kao, H.-E.; Lin, S. H.; Lin, I. J. B. C-H---O Hydrogen Bonds in β-Sheetlike Networks: Combined X-Ray Crystallography and High-Pressure Infrared Study. *J. Am. Chem. Soc.* **2003,** *125*, 12358-12364.
76. Horowitz, S.; Trievel, R. C. Carbon-Oxygen Hydrogen Bonding in Biological Structure and Function. *J. Biol. Chem.* **2012,** *287*, 41576-41582.
77. Trievel, R. C.; Flynn, E. M.; Houtz, R. L.; Hurley, J. H. Mechanism of Multiple Lysine Methylation by the Set Domain Enzyme Rubisco Lsmt. *Nature Struct. Biol.* **2003,** *10*, 545-552.
78. Couture, J.-F.; Dirk, L. M. A.; Brunzelle, J. S.; Houtz, R. L.; Trievel, R. C. Structural Origins for the Product Specificity of Set Domain Protein Methyltransferases. *Proc. Nat. Acad. Sci., USA* **2008,** *105*, 20659-20664.
79. Horowitz, S.; Yessleman, J. D.; Al-Hashimi, H. M.; Trievel, R. C. Direct Evidence for Methyl Group Coordination by Carbon-Oxygen Hydrogen Bonds in the Lysine Methyltransferase Set7/9. *J. Biol. Chem.* **2011,** *286*, 18658-18663.
80. Horowitz, S.; Dirk, L. M. A.; Yesselman, J. D.; Nimtz, J. S.; Adhikari, U.; Mehl, R. A.; Scheiner, S.; Houtz, R. L.; Al-Hashimi, H. M.; Trievel, R. C. Conservation and Functional Importance of Carbon-Oxygen Hydrogen Bonding in Adomet-Dependent Methyltransferases. *J. Am. Chem. Soc.* **2013,** *135*, 15536-15548.

81. Frisch, M. J.; Trucks, G. W.; Schlegel, H. B.; Scuseria, G. E.; Robb, M. A.; Cheeseman, J. R.; Scalmani, G.; Barone, V.; Mennucci, B.; Petersson, G. A., et al. *Gaussian 09*, Revision B.01; Wallingford, CT, 2009.
82. Boys, S. F.; Bernardi, F. The Calculation of Small Molecular Interactions by the Differences of Separate Total Energies. Some Procedures with Reduced Errors. *Mol. Phys.* **1970,** *19*, 553-566.
83. Reed, A. E.; Weinhold, F. Natural Bond Orbital Analysis of near Hartree-Fock Water Dimer. *J. Chem. Phys.* **1983,** *78*, 4066-4073.
84. Weinhold, F. Natural Bond Orbital Analysis: A Critical Overview of Relationships to Alternative Bonding Perspectives. *J. Comput. Chem.* **2012,** *33*, 2363-2379.
85. Bader, R. F. W. *Atoms in Molecules, A Quantum Theory*. Clarendon Press: Oxford, 1990; Vol. 22, p 438.
86. Carroll, M. T.; Bader, R. F. W. An Analysis of the Hydrogen Bond in Base-HF Complexes Using the Theory of Atoms in Molecules. *Mol. Phys.* **1988,** *65*, 695-722.
87. Adhikari, U.; Scheiner, S. The Magnitude and Mechanism of Charge Enhancement of CH··O H-Bonds. *J. Phys. Chem. A* **2013,** *117*, 10551-10562.
88. Scheiner, S. The Interplay between Charge Transfer, Rehybridization, and Atomic Charges in the Internal Geometry of Subunits in Noncovalent Interactions. *Int. J. Quantum Chem.* **2015,** *115*, 28-33.
89. Scheiner, S. Analysis of Catalytic Mechanism of Serine Proteases. Viability of Ring-Flip Hypothesis. *J. Phys. Chem. B* **2008,** *112*, 6837-6846.
90. Nepal, B.; Scheiner, S. Effect of Ionic Charge on the CH···π Hydrogen Bond. *J. Phys. Chem. A* **2014,** *118*, 9575-9587.
91. Weinhold, F.; Schleyer, P. v. R.; McKee, W. C. Bay-Type H···H "Bonding" in Cis-2-Butene and Related Species: QTAIM Versus NBO Description. *J. Comput. Chem.* **2014,** *35*, 1499–1508.
92. Johnson, E. R.; Keinan, S.; Mori-Sanchez, P.; Contreras-Garcia, J.; Cohen, A. J.; Yang, W. Revealing Noncovalent Interactions. *J. Am. Chem. Soc.* **2010,** *132*, 6498-6506.
93. Cormanich, R. A.; Rittner, R.; O'Hagan, D.; Bühl, M. Analysis of CF···FC Interactions on Cyclohexane and Naphthalene Frameworks. *J. Phys. Chem. A* **2014,** *118*, 7901-7910.
94. Azofra, L. M.; Scheiner, S. Complexes Containing CO_2 and SO_2. Mixed Dimers, Trimers and Tetramers. *Phys. Chem. Chem. Phys.* **2014,** *16*, 5142-5149.
95. Foroutan-Nejad, C.; Shahbazian, S.; Marek, R. Toward a Consistent Interpretation of the QTAIM: Tortuous Link between Chemical Bonds, Interactions, and Bond/Line Paths. *Chem. Eur. J.* **2014,** *20*, 10140-10152.
96. Alkorta, I.; Sanchez-Sanz, G.; Elguero, J. Pnicogen Bonds between X=PH_3 (X = O, S, NH, CH_2) and Phosphorus and Nitrogen Bases. *J. Phys. Chem. A* **2014,** *118*, 1527-1537.
97. Varadwaj, P. R.; Varadwaj, A.; Jin, B.-Y. Significant Evidence of CO and Cc Long-Range Contacts in Several Heterodimeric Complexes of CO with CH_3-X, Should One Refer to Them as Carbon and Dicarbon Bonds! *Phys. Chem. Chem. Phys.* **2014,** *16*, 17238-17252.
98. Azofra, L. M.; Scheiner, S. Complexation of n SO_2 Molecules (n=1,2,3) with Formaldehyde and Thioformaldehyde. *J. Chem. Phys.* **2014,** *140*, 034302.

Table 1. Computed binding energies (kcal/mol) for complexes between NMA and indicated electron acceptors, including counterpoise correction

	O··SC	O··SF	SH··O	CH··O	O··C tetrel
$(CH_3)_3S^+$	19.81[a]	-	-	16.30[b] 20.55[c]	13.72
$CH_3SH_2^+$	21.95[d]	-	29.24[e]	18.33[b]	16.03
CH_3SH	1.14[d,f]	-	4.12	1.67[b]	1.90
$FHSCH_3^+$	23.43[d]	39.03	34.09[g]	21.17[b]	17.31[h]
$FSCH_3$	2.71	6.40	-	3.29[b]	2.50[h]

[a]may also contain CH··O [b]linear CH··O
[c]trifurcated: 3 different CH_3 groups [d]fix O··S-C=180°
[e]fix r(SH)=1.36 Å [f]hold SH at fixed dihedral angle
[g]fix r(SH)=1.364 Å [h]fix O··C-S = 179.8°

Table 2. NBO values of E(2) (kcal/mol) computed at the M06-2X/aug-cc-pVDZ level, with secondary interactions in parentheses

	O··SC	O··SF	SH··O	CH··O	O··C tetrel
$(CH_3)_3S^+$	2.16 (2x2.45)[a]	-	-	12.56[b] (1.21)[c]	2.59 (0.46)[d]
$CH_3SH_2^+$	5.66	-	73.36 (3.28)[e]	14.45	3.72
CH_3SH	0.89	-	9.33	2.85 (1.39)[f]	0.73
$FHSCH_3^+$	5.87 (1.71)[g]	62.97 (3.77)[h]	96.63 (3.98)[e]	22.37 (2.75)[i]	3.92
$FSCH_3$	0.80[j] (1.79)[k]	3.55 (2.44)[l]	-	5.99	0.73

[a]$O_{lp} \rightarrow \sigma^*CH + \pi(CO) \rightarrow \sigma^*CH$ [b]single linear CH··O arrangement
[c]$O_{lp} \rightarrow \sigma^*CH$ to second CH [d]$O_{lp} \rightarrow \sigma^*CH$
[e]$OC \rightarrow \sigma^*SH$ [f]$OC \rightarrow \sigma^*CH$ [g]$O_{lp} \rightarrow \sigma^*SF$
[h]$O_{lp} \rightarrow \sigma^*SH$ [i]$S_{lp} \rightarrow \sigma^*CH$ [j]$\pi(CO) \rightarrow \sigma^*SC$
[k]$S_{lp} \rightarrow \sigma^*(CH)$ and $F_{lp} \rightarrow \pi^*(CO)$
[l]$O_{lp} \rightarrow \sigma^*SF + O_{lp} \rightarrow \sigma^*CH + S_{lp} \rightarrow \sigma^*CH$

Table 3. Electron density ρ (au) at AIM bond critical points.

	O··SC	O··SF	SH··O	CH··O	O··C tetrel
$(CH_3)_3S^+$	0.0137 2(0.0151)[a]	-	-	0.0249 0.0066[a]	0.0140
$CH_3SH_2^+$	0.0235	-	0.0697	0.0273	0.0137
CH_3SH	0.0067 2(0.0047)[a]	-	0.0192 0.0053[b]	0.0143 0.0043[c]	0.0062
$FHSCH_3^+$	0.0286	0.0729	0.0891	0.0347	0.0145
$FSCH_3$	0.0094 0.0074[d] 0.0035[e] 0.0043[f]	0.0161 0.0115[a] 0.0066[e]	-	0.0168	0.0068

[a]CH··O [b]SH··C [c]CH···HC
[d]F··C [e]CH··S [f]CH··F

Table 4. Laplacian of electron density $\nabla^2\rho$ (au) at AIM bond critical points

	O··SC	O··SF	SH··O	CH··O	O··C tetrel
$(CH_3)_3S^+$	0.0548 2x(0.0575)[a]	-	-	0.1041 0.0251[a]	0.0639
$CH_3SH_2^+$	0.0972	-	0.1845	0.1188	0.0753
CH_3SH	0.0248 2x(0.0173)[a]	-	0.0651 0.0240[b]	0.0452 0.0161[c]	0.0290
$FHSCH_3^+$	0.0165	0.1332	0.1477	0.1507	0.0785
$FSCH_3$	0.0342 0.0409[d] 0.0142[e] 0.0239[f]	0.0527 0.0423[a] 0.0196[e]	-	0.0469	0.0359

[a]CH··O [b]SH··C [c]CH···HC
[d]F··C [e]CH··S [f]CH··F

Table 5. Change in covalent bond length[a] (mÅ) caused by complexation with NMA

	O···S↔C	O···S↔F	C↔H···O	O···C↔S tetrel
$(CH_3)_3S^+$	2.1	-	4.1	1.4
$CH_3SH_2^+$	-9.8	-	4.8	7.9
CH_3SH	0.6	-	-0.5	2.0
$FHSCH_3^+$	0.6	72.8	17.5	2.0
$FSCH_3$	2.1	20.4	2.4	-1.7

[a]particular bond indicated by ↔

Table 6. Changes in average NMR chemical shift of three methyl protons (ppm) computed at the M06-2X/aug-cc-pVDZ level

	O··SC	O··SF	SH··O	CH··O[a]	O··C tetrel
$(CH_3)_3S^+$	0.34[b]	-	-	-1.16 / -3.74 -0.39 / -2.04[c]	-0.83
$CH_3SH_2^+$	0.58	-	0.33	-1.14 / -4.24	-0.80
CH_3SH	0.13	-	-0.03	-0.52 / -1.10	-0.40
$FHSCH_3^+$	0.57	0.08 (-0.47)[d]	0.47	-1.52 / -5.20	-0.77
$FSCH_3$	0.15	-0.03 (-0.90)[e]	-	-0.73 / -2.51	-0.43

[a]average followed by individual H-bonding proton

[b]CH_3 group opposite O atom of NMA

[c]trifurcated HB structure 1b

[d]R(H··O)=2.33 Å

[3]R(H··O)=2.40 Å

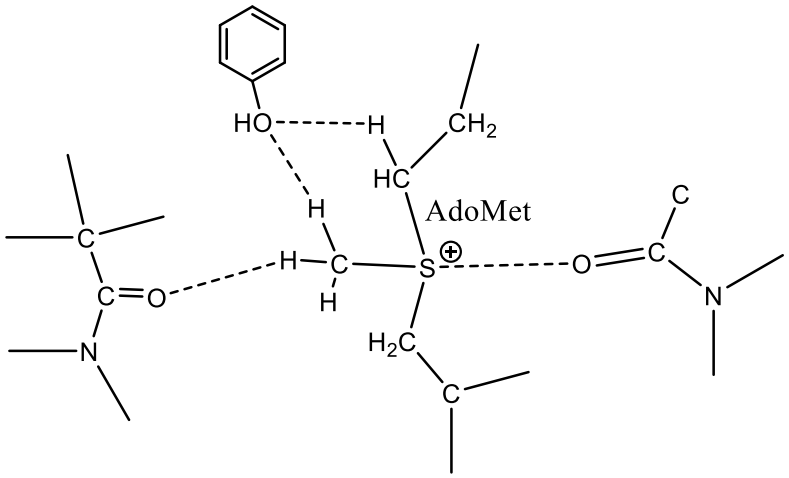

Scheme 1. Diagram of possible H-bonds or chalcogen bonds formed by AdoMet with neighboring groups.

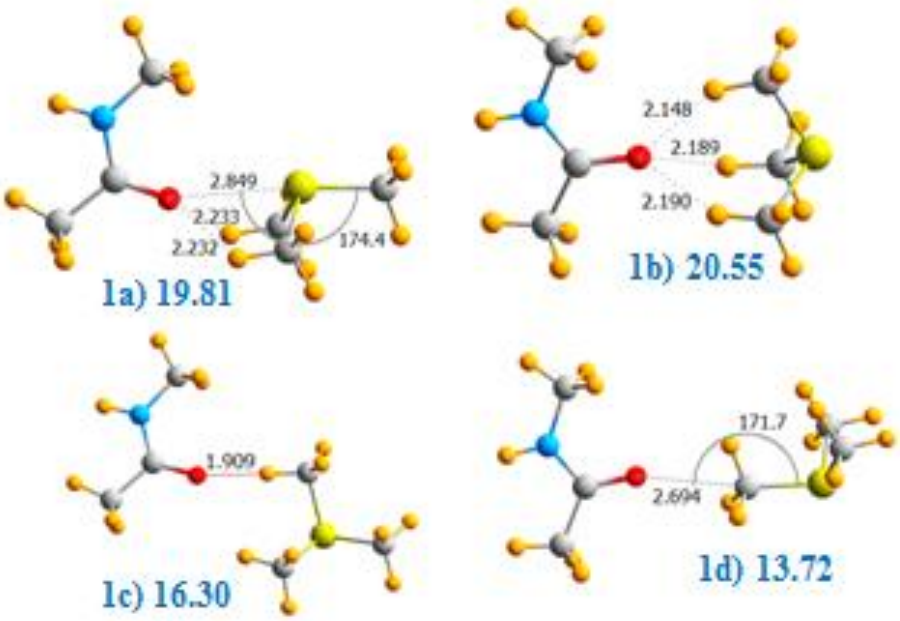

Fig 1. Optimized geometries of complexes of NMA with $(CH_3)_3S^+$. Counterpoise-corrected binding energies (kcal/mol) in blue, distances in Å, angles in degs.

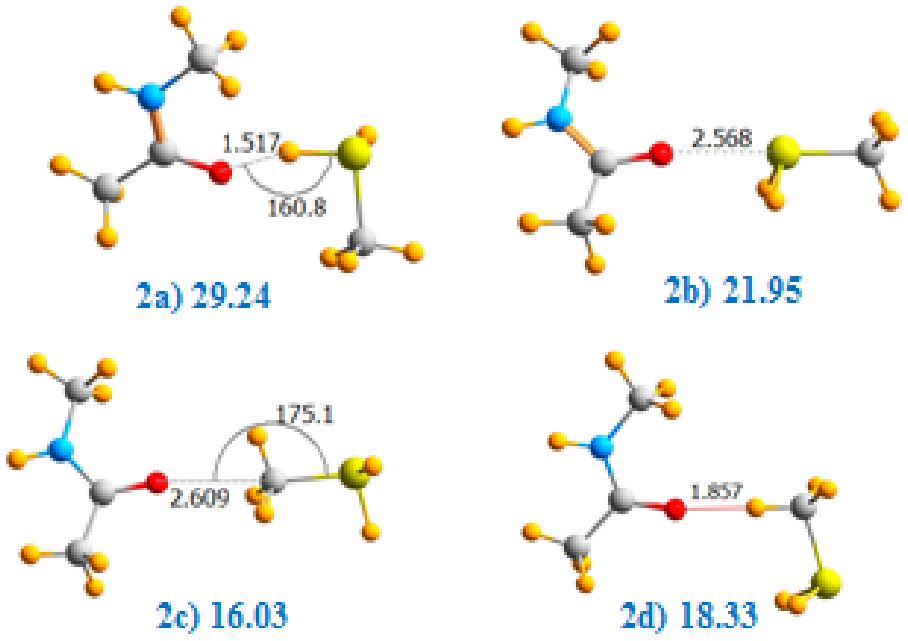

Fig 2. Optimized geometries of complexes of NMA with $CH_3SH_2^+$. Counterpoise-corrected binding energies (kcal/mol) in blue, distances in Å, angles in degs.

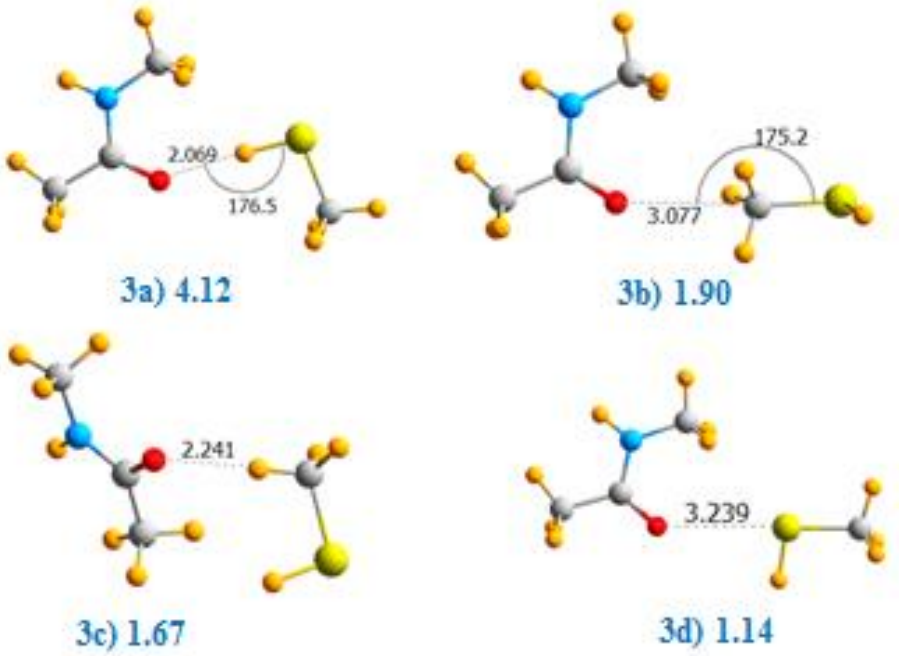

Fig 3. Optimized geometries of complexes of NMA with CH_3SH. Counterpoise-corrected binding energies (kcal/mol) in blue, distances in Å, angles in degs.

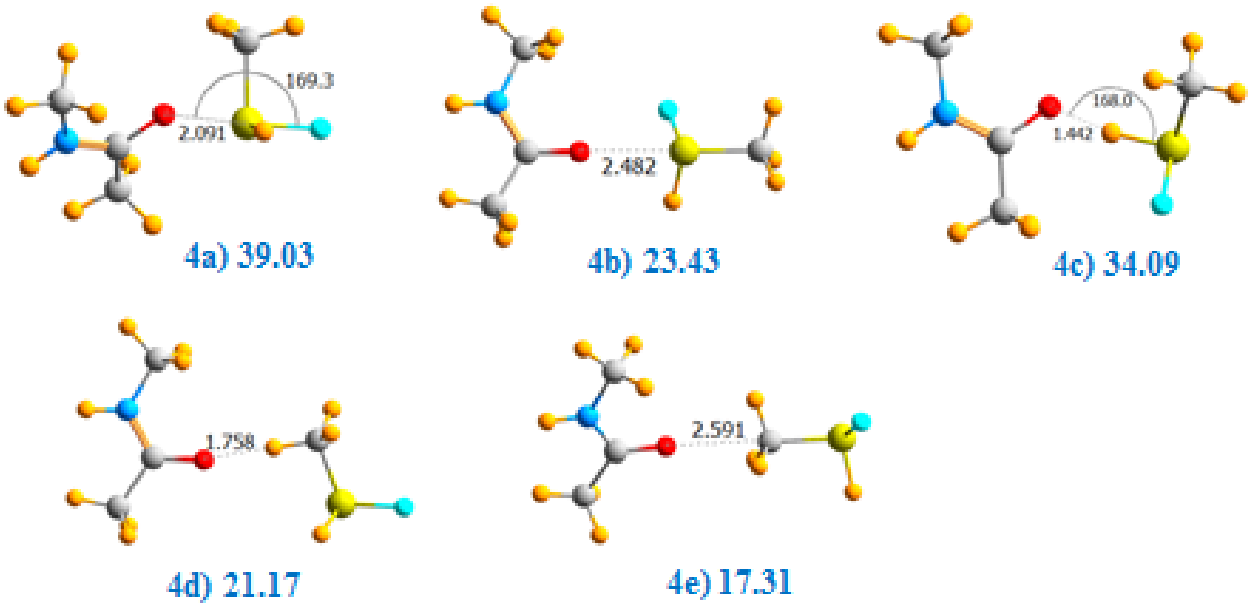

Fig 4. Optimized geometries of complexes of NMA with $FHSCH_3^+$. Counterpoise-corrected binding energies (kcal/mol) in blue, distances in Å, angles in degs.

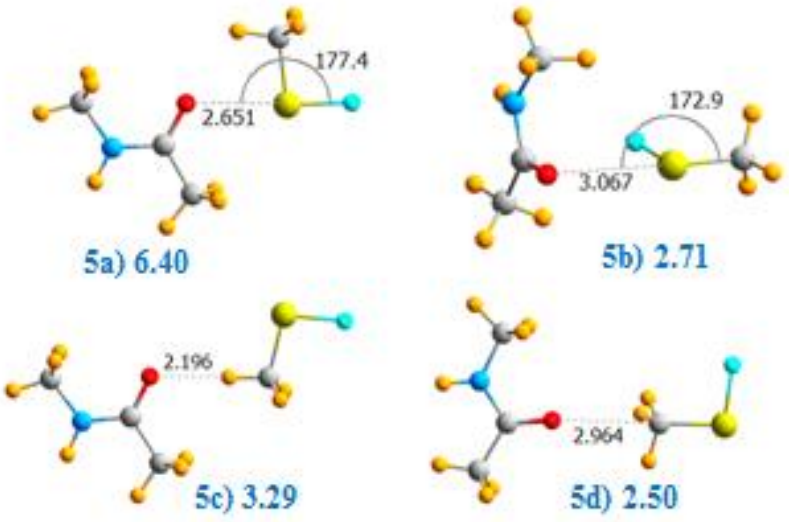

Fig 5. Optimized geometries of complexes of NMA with $FSCH_3$. Counterpoise-corrected binding energies (kcal/mol) in blue, distances in Å, angles in degs.

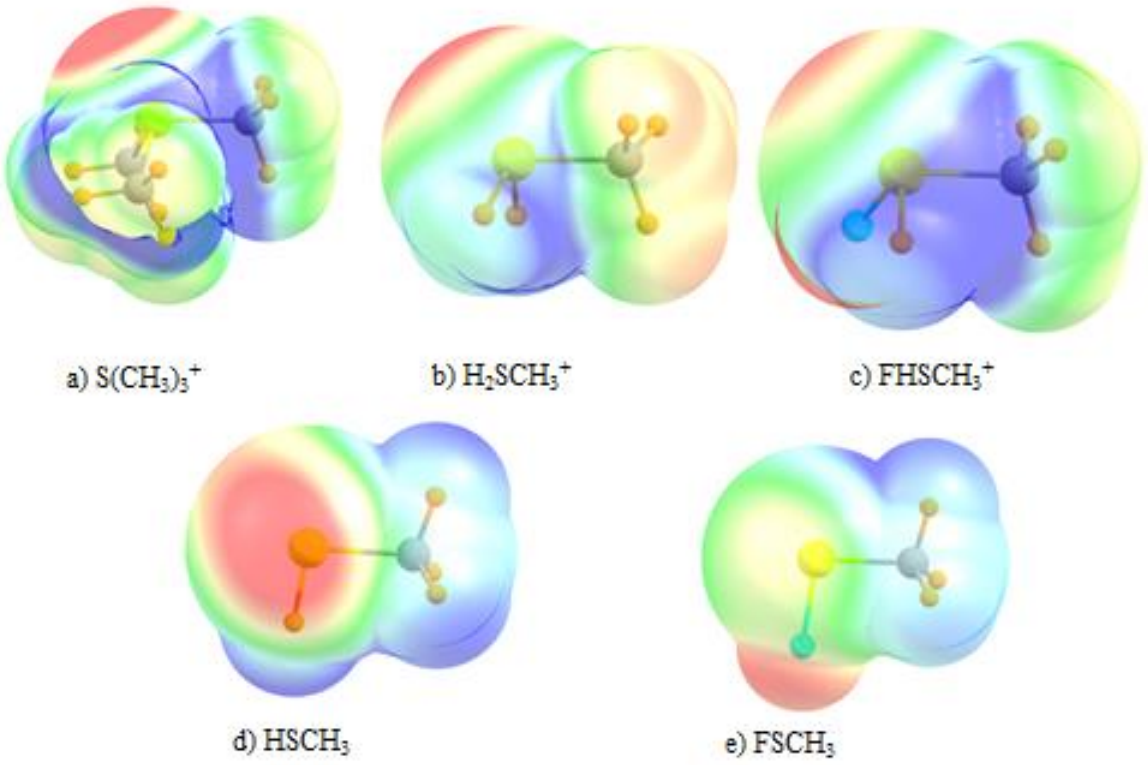

Fig 6. Molecular electrostatic potentials on surface corresponding to 1.5 x the van der Waals radii. Blue/red indicates most positive/negative potentials. Extrema correspond to a) 0.16 - 0.20, b and c) 0.18 - 0.25, d) ±0.03, e) ±0.05 au.

TOC graphic

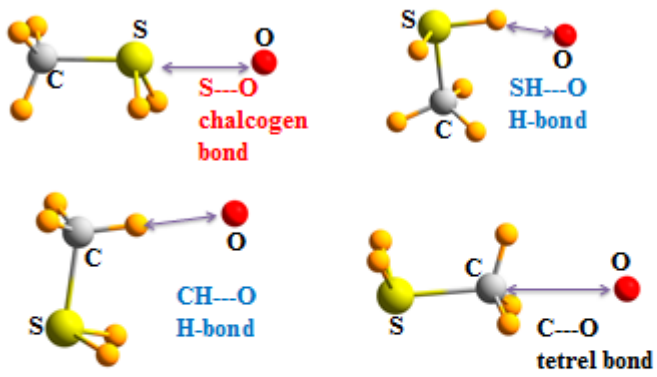
S
O
C
S---O
chalcogen
bond
S
O
C
SH---O
H-bond
C
O
S
CH---O
H-bond
C
O
S
C---O
tetrel bond